World Applied Sciences Journal 32 (9): 1942-1951, 2014
ISSN 1818-4952

DOI: 10.5829/idosi.wasj.2014.32.09.1115

Free Convection Boundary Layer Flow on a Solid Sphere with Convective Boundary Conditions in a Micropolar Fluid

[1]Hamzeh Taha Alkasasbeh, [1]Mohd Zuki Salleh,
[2]Razman Mat Tahar, [3]Roslinda Nazar and [4]Ioan Pop

[1]Futures and Trends Research Group, Faculty of Industrial Science and Technology,
University Malaysia Pahang, 26300 UMP Kuantan, Pahang, Malaysia
[2]Faculty of Technology, Universiti Malaysia Pahang, 26300 UMP Kuantan, Pahang, Malaysia
[3]School of Mathematical Sciences, Faculty of Science and Technology,
Universiti Kebangsaan Malaysia, 43600 UKM Bangi, Selangor, Malaysia
[4]Faculty of Mathematics, University of Cluj, R-3400 Cluj, CP 253, Romania

Abstract: In this paper, the problem of free convection boundary layer flow on a solid sphere in a micropolar fluid with convective boundary conditions, in which heat is supplied through a bounding surface of finite thickness and finite heat capacity is considered. The basic equations of boundary layer are transformed into a non-dimensional form and reduced to nonlinear systems of partial differential equations are solved numerically using an implicit finite difference scheme known as the Keller-box method. Numerical solutions are obtained for the wall temperature, the local heat transfer coefficient and the local skin friction coefficient, as well as the velocity, angular velocity and temperature profiles. The features of the flow and heat transfer characteristics for different values of the material or micropolar parameter, K = 0, (Newtonian fluid), 1, 2, 3, (micropolar fluid), the Prandtl number, Pr = 0.7, 1, 7, the conjugate parameter, γ = 0.05, 0.1,0.2 and the coordinate running along the surface of the sphere, x between 0^o and 120^o are analyzed and discussed.

Key words: Boundary Layer · Convective Boundary Conditions · Free Convection · Micropolar Fluid · Solid Sphere

INTRODUCTION

The essence of the theory of micropolar fluid flow lies in the extension of the constitutive equation for Newtonian fluid, so that more complex fluids such as particle suspensions, liquid crystal, animal blood, lubrication and turbulent shear flows can be described by this theory. The theory of micropolar fluid was first proposed by Eringen [1]. Extensive review of the theory and applications can be found in the review article by Ariman *et al*. [2] and the Blasius boundary-layer flow of a micropolar fluid is considered by Rees and Bassom [3]. On the other hand, Chen and Mucoglu [4] studied the analysis of mixed, forced and free convection about a sphere in a viscous fluid. Further, Nazar *et al*. [5,6,7] considered the free and mixed convection boundary layer flows on a sphere in a viscous and micropolar fluid with constant wall temperature (CWT) and constant heat flux (CHF), respectively. The natural convection heat and mass transfer from a sphere in micropolar fluids with constant wall temperature and concentration were presented by Cheng [8]. On the other hand, the laminar mixed convection boundary layer flow about an isothermal solid sphere in a micropolar fluid was studied by Nazar *et al*. [9]. It should be pointed that all the papers above studied the boundary condition of two cases, i.e. CWT and CHF.

It is worth mentioning that the Newtonian heating conditions in which the heat transfer from the surface is proportional to the local surface temperature have been used by Merkin [10] and Lesnic *et al*. [11-13] where free convection boundary layer flow along vertical and

Corresponding Author: Hamzeh Taha Alkasasbeh, Futures and Trends Research Group, Faculty of Industrial Science and Technology, University Malaysia Pahang, 26300 UMP Kuantan, Pahang, Malaysia.
Tel: +601116851617.

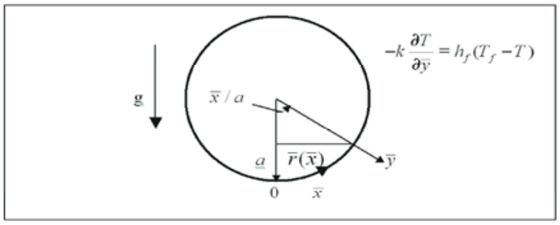

Fig. 1: Physical model and coordinate system

horizontal surfaces in porous medium were studied. Salleh *et al*. [14-17] studied the free and mixed convection boundary layer flows on a sphere with Newtonian heating in viscous and micropolar fluids. On the other hand, Aziz [18] used the convective boundary conditions recently and obtained the similarity solution for laminar thermal boundary layer over a flat plate by applying convective boundary conditions. in which heat is supplied through a bounding surface of finite thickness and finite heat capacity Further, the similarity solutions for flow and heat transfer over a permeable surface and the radiation effects on thermal boundary layer flow over a moving plate with convective boundary conditions have been studied by Ishak [19] and Ishak *et al*. [20]. Merkin and Pop [21] studied the forced convection flow of a uniform stream over a flat surface with a convective surface boundary condition. Yao *et al*. [22] presented the heat transfer of a viscous fluid flow over a stretching/shrinking sheet with a convective boundary condition. Recently, the numerical solution for stagnation point flow over a stretching surface with convective boundary conditions using the shooting method. has been studied by Mohamed *et al*. [23].

Therefore, based on the above-mentioned studies, the aim of the present paper is to study the free convection boundary layer flow on a solid sphere in a micropolar fluid with convective boundary conditions. The governing boundary layer equations are first transformed into a system of non-dimensional equations via non-dimensional variables and then, into non-similar equations before they are solved numerically by the Keller box method as described in the book by Cebeci and Bradshaw [24]. To the best of our knowledge, this present problem (for the case of convective boundary condition) has not been presented before, so the reported results are new.

Basic Eguations: A heated sphere of radius a, which is immersed in a viscous and incompressible micropolar fluid of ambient temperature T_∞, which is subjected to convective boundary conditions (CBC) is considered as shown in Figure 1.

The gravity vector, g acts downward in the opposite direction, whereas the coordinates $\bar{x}$ and $\bar{y}$ are chosen such that $\bar{x}$ measures the distance along the surface of the sphere from the lower stagnation point and $\bar{y}$ measures the distance normal to the surface of the sphere.

We assume that the equations are subjected to convective boundary conditions (CBC) of the form proposed by Aziz [18]. Under the Boussinesq and boundary layer approximations, the basic dimensional equations of the flow are (see Eringen [1] and Salleh *et al*. [16]).

$$\frac{\partial}{\partial \bar{x}}(\bar{r}\,\bar{u}) + \frac{\partial}{\partial \bar{y}}(\bar{r}\,\bar{v}) = 0, \tag{1}$$

$$\rho\left(\bar{u}\frac{\partial \bar{u}}{\partial \bar{x}} + \bar{v}\frac{\partial \bar{u}}{\partial \bar{y}}\right) = (\mu+\kappa)\frac{\partial^2 \bar{u}}{\partial \bar{y}^2} + \rho g\beta(T - T_\infty)\sin\left(\frac{\bar{x}}{a}\right) + \kappa\frac{\partial \bar{H}}{\partial \bar{y}}, \tag{2}$$

$$\rho j\left(\bar{u}\frac{\partial \bar{H}}{\partial \bar{x}} + \bar{v}\frac{\partial \bar{H}}{\partial \bar{y}}\right) = -\kappa\left(2\bar{H} + \frac{\partial \bar{u}}{\partial \bar{y}}\right) + \varphi\frac{\partial^2 \bar{H}}{\partial \bar{y}^2}, \tag{3}$$

$$\bar{u}\frac{\partial T}{\partial \bar{x}} + \bar{v}\frac{\partial T}{\partial \bar{y}} = \frac{\nu}{\Pr}\frac{\partial^2 T}{\partial \bar{y}^2}, \tag{4}$$

subject to the boundary conditions of equations (1) to (4) (see Salleh *et al*. [16]; Aziz [18])

$$\bar{u} = \bar{v} = 0,\ -k\frac{\partial T}{\partial \bar{y}} = h_f(T_f - T)\ \bar{H} = -n\frac{\partial \bar{u}}{\partial \bar{y}} \ \text{at}\ \bar{y} = 0$$
$$\bar{u} \to 0,\ T \to T_\infty,\ \bar{H} \to 0 \ \text{as}\ \bar{y} \to \infty, \tag{5}$$

where $\bar{u}$ and $\bar{v}$ are the velocity components along the $\bar{x}$ and $\bar{y}$ directions, respectively, $\bar{H}$ is the angular velocity of micropolar fluid, κ is the vortex viscosity, T is the local temperature, T_f is the temperature of the hot fluid, g is the gravity acceleration, β is the thermal expansion coefficient, $v = \mu/\rho$ is the kinematic viscosity, μ is the dynamic viscosity, ρ is the density, j is the microinertia density, Pr is the Prandtl number and h_f is the heat transfer coefficient for the convective boundary conditions It is worth mentioning that in boundary conditions (5), n is constant and $0 \le n \le 1$. The value n=0, which leads to $\bar{H} = 0$ at the wall, represents concentrated particle flows in which the particle density is sufficiently great that microelements close to the wall are unable to rotate or is called "strong" concentration of microelements [25, 26]. The case corresponding to $n = 1$ results in the vanishing of antisymmetric part of the stress tensor and represents "weak" concentration of microelements [26]. In this case, the particle rotation is equal to fluid vorticity at the boundary for fine particle suspension. When $n = 1$, we have flows which are representative of turbulent boundary layer [27]. The case of $n = 1/2$, is considered in this paper.

Let $\bar{r}(\bar{x})$ be the radial distance from the symmetrical axis to the surface of the sphere and φ is the spin gradient viscosity which are represented by

$$\bar{r}(\bar{x}) = a\,\sin(\bar{x}/a),\ \ \varphi = (\mu + (\kappa/2))\,j \tag{6}$$

We now introduce the following non-dimensional variables (Salleh *et al*. [16]; Aziz [18]):

$$x = \frac{\bar{x}}{a},\ y = Gr^{1/4}\left(\frac{\bar{y}}{a}\right),\ r = \frac{\bar{r}}{a},$$

$$u = \left(\frac{a}{v}\right)Gr^{-1/2}\bar{u},\ v = \left(\frac{a}{v}\right)Gr^{-1/4}\bar{v},\ H = \left(\frac{a^2}{v}\right)Gr^{-3/4}\bar{H},\ \theta = \frac{T - T_\infty}{T_f - T_\infty} \tag{7}$$

where $Gr = g\beta(T_f - T_\infty)\dfrac{a^3}{v^2}$ is the Grashof number for convective boundary conditions.

Substituting variables (7) into (1) to (4) leads to the following non-dimensional equations

$$\frac{\partial}{\partial x}(ru) + \frac{\partial}{\partial y}(rv) = 0, \tag{8}$$

$$u\frac{\partial u}{\partial x} + v\frac{\partial u}{\partial y} = (1+K)\frac{\partial^2 u}{\partial y^2} + \theta\sin x + K\frac{\partial H}{\partial y}, \tag{9}$$

$$u\frac{\partial H}{\partial x} + v\frac{\partial H}{\partial y} = -K\left(2H + \frac{\partial u}{\partial y}\right) + \left(1 + \frac{K}{2}\right)\frac{\partial^2 H}{\partial y^2}, \tag{10}$$

$$u\frac{\partial \theta}{\partial x} + v\frac{\partial \theta}{\partial y} = \frac{1}{\Pr}\frac{\partial^2 \theta}{\partial y^2}, \tag{11}$$

where K is the material or micropolar parameter defined as $K = \frac{\kappa}{\mu}$. The boundary conditions (5) become

$$u = v = 0,\ \frac{\partial \theta}{\partial y} = -\gamma(1-\theta)\ H = -\frac{1}{2}\frac{\partial u}{\partial y}\ \text{at}\ y = 0$$

$$u \to 0,\ \theta \to 0,\ H \to 0\ \text{as}\ y \to \infty \tag{12}$$

where and $\gamma = ah_f Gr^{-1/4}/k$ are the conjugate parameter for convective boundary condition. It is noticed that if we write the boundary condition $\theta = 1 + \frac{\partial\theta/\partial y}{\gamma}$ at $y = 0$ and when $\gamma \to \infty$ we have $\theta = 1$, this mean the convective boundary conditions (CBC) becomes to constant wall temperature (CWT) at $\gamma \to \infty$ this case studied by Nazar *et al* [5].
To solve equations (8) to (11) subjected to the boundary conditions (12), we assume the following variables:

$$\psi = xr(x)f(x,y),\ \theta = \theta(x,y),\ H = xh(x,y), \tag{13}$$

where ψ is the stream function is defined as

$$u = \frac{1}{r}\frac{\partial\psi}{\partial y} \text{ and } v = -\frac{1}{r}\frac{\partial\psi}{\partial x}, \tag{14}$$

which satisfies the continuity equation (8). Substituting (14) into equations (9) to (11) and after some algebraic calculation, we get the following transformed equations

$$(1+K)\frac{\partial^3 f}{\partial y^3} + (1 + x\cot x) f\frac{\partial^2 f}{\partial y^2} - \left(\frac{\partial f}{\partial y}\right)^2 + \frac{\sin x}{x}\theta + K\frac{\partial h}{\partial y} = x\left(\frac{\partial f}{\partial y}\frac{\partial^2 f}{\partial x\partial y} - \frac{\partial f}{\partial x}\frac{\partial^2 f}{\partial y^2}\right), \tag{15}$$

$$\left(1+\frac{K}{2}\right)\frac{\partial^2 h}{\partial y^2} + (1 + x\cot x) f\frac{\partial h}{\partial y} - \frac{\partial f}{\partial y}h - K\left(2h + \frac{\partial^2 f}{\partial y^2}\right) = x\left(\frac{\partial f}{\partial y}\frac{\partial h}{\partial x} - \frac{\partial f}{\partial x}\frac{\partial h}{\partial y}\right), \tag{16}$$

$$\frac{1}{\Pr}\frac{\partial^2\theta}{\partial y^2} + (1 + x\cot x) f\frac{\partial\theta}{\partial y} = x\left(\frac{\partial f}{\partial y}\frac{\partial\theta}{\partial x} - \frac{\partial f}{\partial x}\frac{\partial\theta}{\partial y}\right), \tag{17}$$

subject to the boundary conditions

$$f = \frac{\partial f}{\partial y} = 0,\ \frac{\partial\theta}{\partial y} = -\gamma(1-\theta),\ h = -\frac{1}{2}\frac{\partial^2 f}{\partial y^2} \text{ at } y = 0$$

$$\frac{\partial f}{\partial y} \to 0,\ \theta \to 0,\ h \to 0, \text{ as } y \to \infty \tag{18}$$

At the lower stagnation point of the sphere, $x \approx 0$, equations (15) to (17) reduce to the following nonlinear ordinary differential equations:

$$(1+K)f''' + 2ff'' - f'^2 + \theta + Kh' = 0 \tag{19}$$

$$\left(1+\frac{K}{2}\right)h'' + 2fh' - f'h - K(2h + f'') = 0 \tag{20}$$

$$\frac{1}{\Pr}\theta'' + 2f\theta' = 0 \tag{21}$$

and the boundary conditions (18) become

$$f(0) = f'(0) = 0,\ \theta'(0) = -\gamma(1-\theta(0)),\ h(0) = -\frac{1}{2}f''(0),$$

$$f' \to 0, \theta \to 0,\ h \to 0 \text{ as } y \to \infty \tag{22}$$

along with $\theta'(0) = -\gamma(1+\theta(0))$ (NH).
where primes denote differentiation with respect to y. The physical quantities of interest in this problem are the local skin friction coefficient, C_f and the local heat transfer coefficient, Q_w(x) which are given by

$$C_f = \left(1+\frac{K}{2}\right)x\frac{\partial^2 f}{\partial y^2}(x,0),\ Q_w(x) = \gamma(1-\theta(x,0)) \tag{23}$$

where $C_f = \tau_w/(\rho U_\infty{}^2)$ is the skin friction coefficient and $\tau_w = [(\mu+\kappa)(\partial\bar{u}/\partial\bar{y}) + \kappa H]_{\bar{y}=0}$ is the wall shear stress. At the lower stagnation point of the sphere, $x \approx 0$, the skin friction coefficient and the heat transfer coefficient are measured by $\frac{\partial^2 f}{\partial y^2}$ and $-\frac{\partial\theta}{\partial y}$, respectively.

RESULTS AND DISCUSSION

The nonlinear systems of partial differential equations (15) to (17) subject to the boundary conditions

Table 1: Values of the wall temperature $\theta(0, y)$ for various values of K when Pr = 0.7, 1, 7 and $\gamma = 1$ (NH)

Pr	0.7		1		7	
K	Salleh *et al* [16]	Present	Salleh *et al*. [16]	Present	Salleh *et al*. [16]	Present
0	26.4584	26.457843	17.2861	17.286076	3.3651	3.365051
1	38.3841	38.384234	25.2867	25.286700	4.6309	4.630875
2	49.1395	49.139487	32.4395	32.439465	5.5150	5.515012
3	59.3500	59.350021	39.2872	39.287163	6.4152	6.415192

Table 2: Values of the wall temperature $\theta(0, y)$ and the skin friction coefficient $\frac{\partial^2 f}{\partial y^2}(0,y)$ for various values of K when Pr= 0.7 and γ = 0.05,0.1,0.2

	0.05 Present		0.1 Present		0.2 Present	
K	$\theta(0, y)$	$\frac{\partial^2 f}{\partial y^2}(0,y)$	$\theta(0, y)$	$\frac{\partial^2 f}{\partial y^2}(0,y)$	$\theta(0, y)$	$\frac{\partial^2 f}{\partial y^2}(0,y)$
0	0.149501	0.184661	0.238308	0.262053	0.360667	0.357656
1	0.157545	0.133231	0.251021	0.183022	0.378091	0.244051
2	0.162725	0.111617	0.259056	0.149459	0.388925	0.195632
3	0.166740	0.099368	0.265189	0.130425	0.397069	0.168159

(18) are solved numerically using the Keller-box method for the case of convective boundary conditions (CBC) with four parameters considered, namely the material parameter K, the Prandtl number Pr, the conjugate parameter γ and the coordinate running along the surface of the sphere, x.

The numerical solution starts at the lower stagnation point of the sphere, $x \approx 0$ and proceeds around the sphere up to the point of $x = 120°$. Values of K considered are K = 0 (Newtonian fluid), 1, 2, 3 (micropolar fluid) and values of Pr considered are Pr = 0.7, 1, 7 at different positions $0° \leq x \leq 120°$. It is worth mentioning that small values of Pr(<<1) physically correspond to liquid metals, which have high thermal conductivity but low viscosity, while large values of Pr(>>1) correspond to high-viscosity oils. It is worth pointing out that specifically, Prandtl numbers Pr = 0.7, 1, 7 correspond to air, electrolyte solution such as salt water and water, respectively.

The values of the wall temperature $\theta(0,y)$ for the values of K = 0, 1, 2, 3 when Pr = 0.7, 1, 7 and $\gamma = 1$ in the case of Newtonian heating (NH) are shown in Table 1. In order to verify the accuracy of the present method, the present results are compared with those reported by Salleh *et al*. [16]. It is found that the agreement between the previously published results with the present ones is very good.

Table 2 shows the values of the wall temperature, $\theta(0, y)$ and the skin friction coefficient, $\frac{\partial^2 f}{\partial y^2}(0,y)$ for various values of K when Pr= 0.7 and γ = 0.05,0.1,0.2. It is found that for fixed γ, as K increases, the values of $\theta(0,y)$ increase but the values of $\frac{\partial^2 f}{\partial y^2}(0,y)$ decrease. Also, it is found that for fixed K, as γ increases, both $\theta(0, y)$ and $\frac{\partial^2 f}{\partial y^2}(0,y)$ increase.

Tables 3 to 5 show the values of the wall temperature $\theta(0, y)$, the heat transfer coefficient $-\frac{\partial \theta}{\partial y}(0,y)$ and the skin friction coefficient $\frac{\partial^2 f}{\partial y^2}(0,y)$ for various values of K when Pr = 0.7, 1, 7 and $\gamma = 0.1$. It is found that for fixed Pr, as K increases, the value of $\theta(0, y)$ increase but the values of $-\frac{\partial \theta}{\partial y}(0,y)$ and $\frac{\partial^2 f}{\partial y^2}(0,y)$ decrease. Also, it is found that for fixed K, as Pr increases, both $\theta(0, y)$ and $\frac{\partial^2 f}{\partial y^2}(0,y)$ decrease but $-\frac{\partial \theta}{\partial y}(0,y)$ increase. From these tables, the values of $\theta(0, y)$ are higher for micropolar fluid ($K \neq 0$) than those for Newtonian fluid (K = 0) but the values of $-\frac{\partial \theta}{\partial y}(0,y)$ and $\frac{\partial^2 f}{\partial y^2}(0,y)$ are lower for micropolar fluid ($K \neq 0$) than those for Newtonian fluid (K = 0).

Tables 6 to 9 present the values of the local heat transfer coefficient $Q_w(x)$ and the local skin friction coefficient C_f for various values of x when Pr = 0.7, 1, 7,

Table 3: Values of the wall temperature $\theta(0, y)$ for various values of K when Pr = 0.7, 1, 7 and γ = 0.1

Pr	0.7	1	7
K	Present	Present	Present
0	0.238308	0.219728	0.144616
1	0.251021	0.232412	0.153825
2	0.259056	0.240367	0.159325
3	0.265189	0.246400	0.163335

Table 4: Values of the heat transfer coefficient $-\frac{\partial \theta}{\partial y}(0, y)$ for various values of K when Pr = 0.7, 1, 7 and γ = 0.1

Pr	0.7	1	7
K	Present	Present	Present
0	0.076169	0.078027	0.085538
1	0.074898	0.076759	0.084617
2	0.074094	0.075963	0.084067
3	0.073481	0.075360	0.083666

Table 5: Values of the skin friction coefficient $\frac{\partial^2 f}{\partial y^2}(0, y)$ for various values of K when Pr = 0.7, 1, 7 and γ = 0.1

	0.7	1	7
Pr K	Present	Present	Present
0	0.262053	0.232622	0.118772
1	0.183022	0.163781	0.089184
2	0.149459	0.134749	0.077445
3	0.130425	0.118279	0.070782

Table 6: Values of the local heat transfer coefficient $Q_w(x)$ for various values of x when Pr = 0.7, 1 and 7, K = 0 and γ = 0.5

	0.7	1	7
Pr x	Present	Present	Present
0°	0.330798	0.332928	0.360684
10°	0.323643	0.327921	0.358815
20°	0.323202	0.327438	0.358336
30°	0.322499	0.326561	0.357508
40°	0.321294	0.325299	0.356348
50°	0.319768	0.323628	0.354863
60°	0.317876	0.321551	0.352915
70°	0.315431	0.318872	0.350475
80°	0.312381	0.315538	0.347495
90°	0.308578	0.311404	0.343626
100°	0.303817	0.306267	0.338416
110°	0.297992	0.300045	0.332281
120°	0.290076	0.291707	0.324164

Table 7: Values of the local skin friction coefficient, C_f for various values of x when Pr = 0.7, 1, 7, K = 0 and γ = 0.5

	0.7	1	7
Pr x	Present	Present	Present
0°	0.000000	0.000000	0.000000
10°	0.034291	0.032424	0.019232
20°	0.068051	0.064377	0.038208
30°	0.100840	0.095508	0.056746
40°	0.132223	0.125369	0.074045
50°	0.161811	0.153571	0.091395
60°	0.188384	0.179001	0.106634
70°	0.213152	0.202794	0.120807
80°	0.235005	0.223868	0.133682
90°	0.253596	0.241800	0.144351
100°	0.268672	0.256273	0.153816
110°	0.279600	0.266518	0.160617
120°	0.286714	0.272626	0.164811

Table 8: Values of the local heat transfer coefficient Q_w(ix) for various values of x when Pr = 0.7, 1, 7, K = 2 and γ = 0.5

	0.7	1	7
Pr x	Present	Present	Present
0°	0.318250	0.322975	0.386933
10°	0.317922	0.322470	0.381694
20°	0.317658	0.322153	0.381362
30°	0.317211	0.321659	0.380709
40°	0.316598	0.320812	0.379754
50°	0.315804	0.319797	0.378451
60°	0.314858	0.318588	0.376841
70°	0.313697	0.317094	0.374693
80°	0.312337	0.315328	0.372073
90°	0.310761	0.313264	0.368721
100°	0.308944	0.310862	0.364647
110°	0.306907	0.308146	0.359724
120°	0.302652	0.304752	0.353513

Table 9: Values of the local skin friction coefficient, C_f for various values of x when Pr = 0.7, 1, 7, K = 2 and γ = 0.5

	0.7	1	7
Pr x	Present	Present	Present
0°	0.000000	0.000000	0.000000
10°	0.063458	0.062299	0.047452
20°	0.126326	0.124072	0.094862
30°	0.188080	0.184866	0.142196
40°	0.248124	0.244147	0.189483
50°	0.305980	0.301498	0.236618
60°	0.359604	0.354889	0.282270
70°	0.411721	0.407061	0.329185
80°	0.460355	0.456068	0.375692
90°	0.505152	0.501525	0.422065
100°	0.545910	0.543212	0.467708
110°	0.581465	0.579857	0.511386
120°	0.627322	0.614398	0.556060

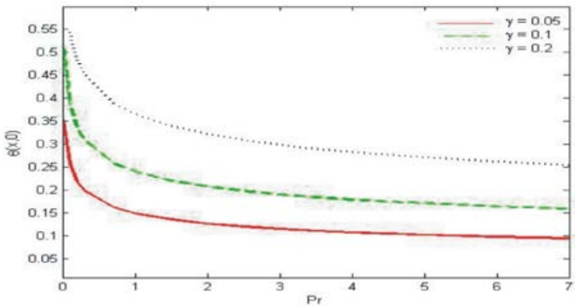

Fig. 2: Variation of wall temperature, $\theta(x, 0)$ with Prandtl number Pr when $K = 2$ and $\gamma = 0.0.5$, 0.1, 0.2

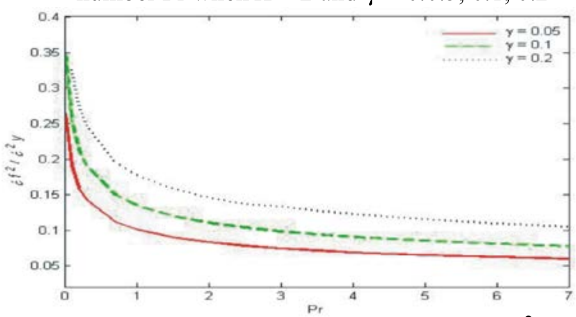

Fig. 3: Variation of the skin friction coefficient, $\frac{\partial^2 f}{\partial y^2}(x,0)$ with Prandtl number Pr when $K = 2$ and $\gamma = 0.05$, 0.1, 0.2.

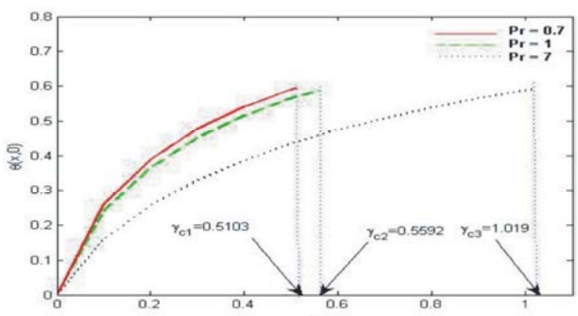

Fig. 4: Variation of wall temperature, $\theta(x, 0)$ with conjugate parameter γ when Pr =0.7, 1, 7 and $K = 2$

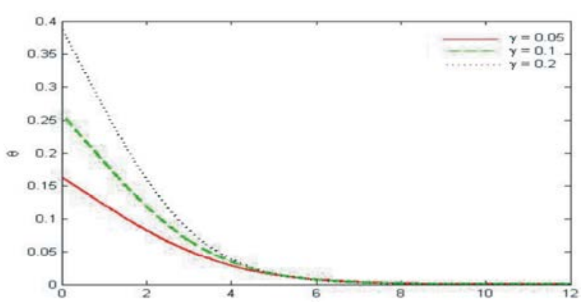

Fig. 5: Temperature profiles $\theta(0, x)$ for some values of γ = 0.0.5, 0.1, 0.2 when Pr= 0.7 and $K = 2$

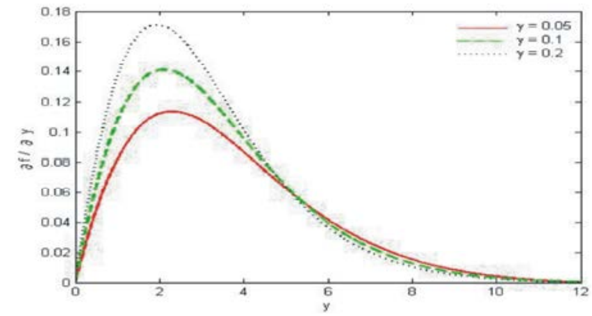

Fig. 6: Velocity profiles $\frac{\partial f}{\partial y}(0,y)$ for some values of γ = 0.05, 0.1, 0.2 when Pr= 0.7 and $K = 2$

$K = 0$, 2 and $\gamma = 0.5$, respectively. It is found that, for fixed K, as Pr increases, the $Q_w(x)$ increase and C_f decrease. From these tables, for a fixed Pr, as x increases, i.e. from the lower stagnation point of the sphere, $x \approx 0$ and proceeds around the sphere up to the point $x = 120°$, the values of $Q_w(x)$ decrease and C_f increase. On the other hand, the values of C_f are higher for micropolar fluid ($K = 2$) than those for Newtonian fluid ($K = 0$).

The graphs of $\theta(x, 0)$ and $\frac{\partial^2 f}{\partial y^2}(x,0)$ for some values of the Prandtl number Pr when $\gamma = 0.05$, 0.1 and 0.2 are plotted in Figures 2 and 3, respectively. It is found that, as Pr increases, both $\theta(x, 0)$ and $\frac{\partial^2 f}{\partial y^2}(x,0)$ decrease. For small values of Pr(<<1), the value of $\theta(x, 0)$ and $\frac{\partial^2 f}{\partial y^2}(x,0)$ is higher than for large values of Pr(>>1) and it is seen that the surface temperature is very sensitive to the Prandtl number variations.

Figure 4 illustrates the variation of the wall temperature $\theta(x, 0)$ with conjugate parameter γ when Pr = 0.7, 1, 7 and $K = 2$. Furthermore, in order to get a physically acceptable solution, γ must be less than or equals to some critical value, say γ_c, i.e. $\gamma \le \gamma_c$, depending on Pr. It can be seen from this figure that $\theta(x, 0)$ becomes larger as γ approaches the critical value of $\gamma_{c1} = 0.5103$ when Pr = 0.7, $\gamma_{c2} = 0.5592$ when Pr =1 and $\gamma_{c3} = 1.019$ when Pr = 7.

Figures 5 to 7 illustrate the temperature $\theta(x, 0)$, velocity $\frac{\partial f}{\partial y}(0,y)$ and angular velocity $h(0, y)$ profiles of the sphere for some values of γ, namely $\gamma = 0.05$, 0.1, 0.2 when Pr= 0.7 and $K = 2$, respectively. It is found that when K is fixed, as γ increases, the temperature, velocity and angular velocity profiles increase.

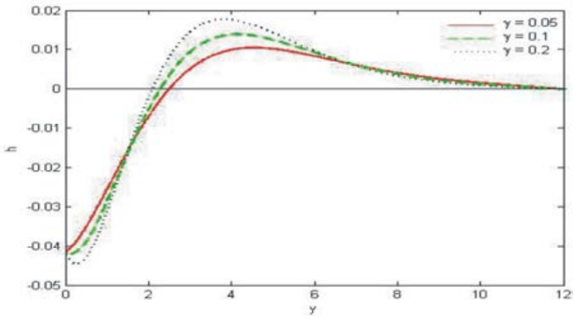

Fig. 7: Angular velocity profiles $h(0, y)$ for some values of $\gamma = 0.05, 0.1, 0.2$ when Pr= 0.7 and $K = 2$

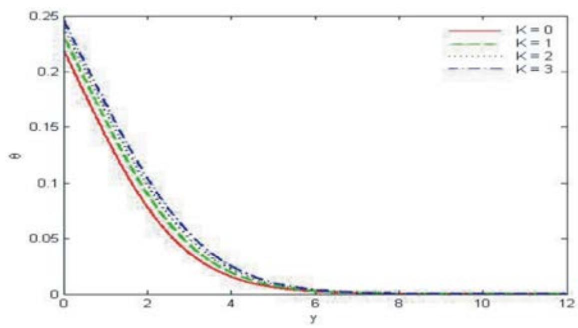

Fig. 8: Temperature profiles, $\theta(0, x)$ when $K = 0, 1, 2, 3$, Pr = 1 and $\gamma = 0.1$

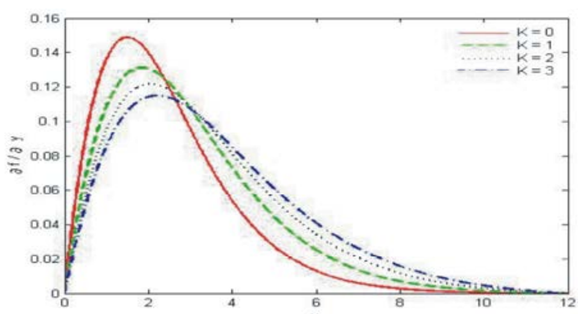

Fig. 9: Velocity profiles, $\frac{\partial f}{\partial y}(0, y)$ when $K = 0, 1, 2, 3$, Pr = 1 and $\gamma = 0.1$

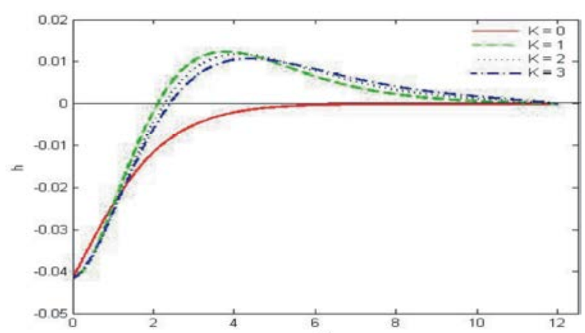

Fig. 10: Angular velocity profiles, $h(0, y)$ when $K = 0, 1, 2, 3$, Pr = 1 and $\gamma = 0.1$

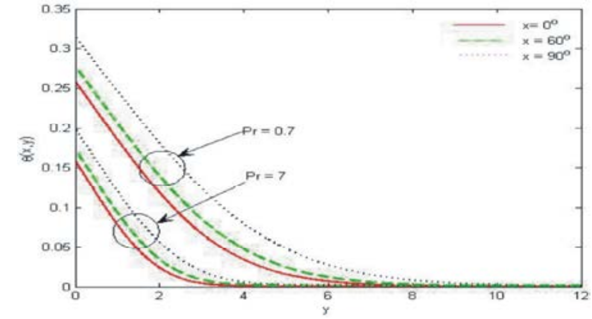

Fig. 11: Temperature profiles, $\theta(x, y)$ at $x = 0°, 60°, 90°$ when Pr = 0.7, 7, $K = 2$ and $\gamma = 0.1$

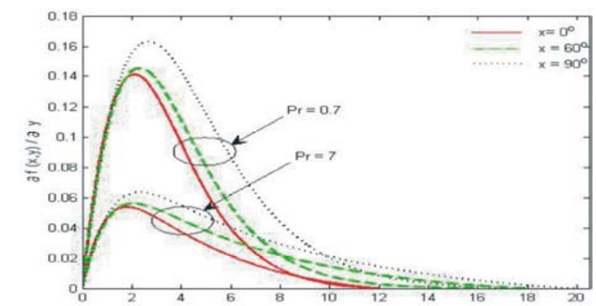

Fig. 12: Velocity profiles, $\frac{\partial f}{\partial y}(x, y)$ at $x = 0°, 60°, 90°$ when Pr = 0.7, 7, $K = 2$ and $\gamma = 0.1$

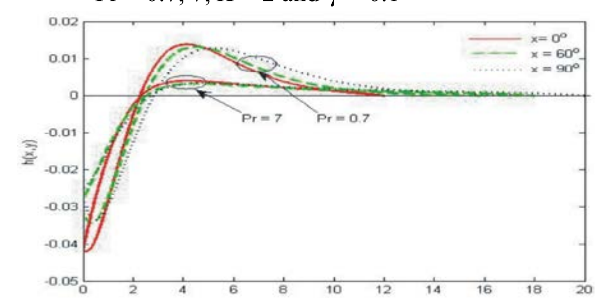

Fig. 13: Angular velocity profiles, $h(x, y)$ at $x = 0°, 60°, 90°$ when Pr = 0.7, 7, $K = 2$ and $\gamma = 0.1$

Figures 8 and 9 display the temperature $\theta(0, y)$ and velocity $\frac{\partial f}{\partial y}(0, y)$ profiles for some values of K, namely $K = 0, 1, 2, 3$ when Pr = 1 and $\gamma = 0.1$, respectively. It is found that when Pr is fixed, as K increases, both the temperature and velocity profiles increase. Angular velocity $h(0, y)$ profiles, when $K = 0, 1, 2, 3$, Pr = 1 and $\gamma = 0.1$ are plotted in Figure 10. These figures shows that the angular velocity is completely negative for $K = 0$, while it may be positive for $K \neq 0$.

Figures 11 to 13 display the temperature, velocity and angular velocity profiles at $x = 0°, 60°, 90°$ when Pr = 0.7, 7, $K = 2$ and $\gamma = 0.1$. From Figure 11, it is found that as Pr and x increase, the temperature profiles decrease and the thermal boundary layer thickness also decrease. This is because for small values of the Prandtl number Pr <<1, the fluid is highly conductive. Physically, if Pr increases, the thermal diffusivity decreases and this phenomenon leads to the decreasing manner of the energy transfer ability that reduces the thermal boundary layer. Furthermore, in these figures shown that for fixed K, as Pr increases, the velocity profiles decrease and the angular velocity profiles decrease. In the same figures it has been found that when Pr is fixed and x increases, the temperature, velocity and angular velocity profiles increase.

CONCLUSIONS

In this paper, we have numerically studied the problem of free convection boundary layer flow on a solid sphere in a micropolar fluid with convective boundary conditions (CBC). We are interested to see how the material parameter K, the Prandtl number Pr and the conjugate parameter γ affect the flow and heat transfer characteristics. We can conclude that (for the case of (CBC):

- When Pr and γ are fixed, as K increases, the value of the wall temperature $\theta(0, y)$ increases but the skin friction coefficient, $\frac{\partial^2 f}{\partial y^2}(0,y)$ decreases. On other hand, when K and γ are fixed, as Pr increases, the heat transfer coefficient, $-\frac{\partial \theta}{\partial y}(0,y)$, the skin friction coefficient, $\frac{\partial^2 f}{\partial y^2}(0,y)$ and the angular velocity profiles, $h(0, y)$ decrease but the heat transfer coefficient $-\frac{\partial \theta}{\partial y}(0,y)$ increases
- When K is fixed, an increase in γ leads to an increase of the wall temperature $\theta(0, y)$ skin friction coefficient $\frac{\partial^2 f}{\partial y^2}(0,y)$, temperature profiles $\theta(0, y)$ velocity profiles $\frac{\partial f}{\partial y}(0,y)$ and angular velocity profiles $h(0, y)$.
- When Pr and γ are fixed, the values of C_f are higher for micropolar fluids ($K \neq 0$) than those for a Newtonian fluid ($K = 0$);
- When Pr is fixed and x increases, the temperature profile, velocity profile and angular velocity profiles increase;
- When K and γ are fixed, as Pr increases, the values of the local heat transfer coefficient increase and the local skin friction coefficient decrease;
- To get a physically acceptable solution, γ must be less than γ_c depending on the Pr.

ACKNOWLEDGEMENT

The authors gratefully acknowledge the financial supports received from the Universiti Malaysia Pahang (RDU 121302 and RDU 120390).

REFERENCES

1. Eringen, A.C., 1966. Theory of micropolar fluid, Journal of Mathematics and Mechanics, 16: 1-18.
2. Ariman, T., M. Turk and N. Sylvester, 1974. Applications of microcontinuum fluid mechanics. International Journal of Engineering Science, 11(8): 905-930.
3. Rees, D.A. and A.P. Basson, 1996. The Blasius boundary layer flow of a micropolar fluid. International Journal of Engineering Science, 34(1): 113-124.
4. Chen, T. and A. Mucoglu, 1977. Analysis of mixed forced and free convection about a sphere. International Journal of Heat and Mass Transfer, 20(8): 867-875.
5. Nazar, R., N. Amin, T. Grosan and I. Pop, 2002a. Free convection boundary layer on an isothermal sphere in a micropolar fluid. International communications in heat and mass transfer, 29(3): 377-386.
6. Nazar, R., N. Amin, T. Grosan and I. Pop, 2002b. Free convection boundary layer on a sphere with constant surface heat flux in a micropolar fluid. International communications in heat and mass Transfer, 29(8): 1129-1138.
7. Nazar, R., N. Amin and I. Pop, 2002c. On the mixed convection boundary-layer flow about a solid sphere with constant surface temperature. Arabian Journal for Science and Engineering, 27(2): 117-135.
8. Cheng, C.Y., 2008. Natural convection heat and mass transfer from a sphere in micropolar fluids with constant wall temperature and concentration. International Communications in Heat and Mass Transfer, 35(6): 750-755.
9. Tham, L. and R. Nazar, 2012. Mixed convection flow about a solid sphere embedded in a porous medium filled with a nanofluid. Sains Malaysiana, 41(12): 1643-1649.
10. Merkin, J., 1994. Natural-convection boundary-layer flow on a vertical surface with Newtonian heating. International Journal of Heat and Fluid Flow, 15(5): 392-398.

11. Lesnic, D., D Ingham and I. Pop, 1999. Freeconvection boundary-layer flow along a vertical surface in a porous medium with Newtonian heating. International Journal of Heat and Mass Transfer, 42(14): 2621-2627.
12. Lesnic, D., D. Ingham and I. Pop, 2000. Free convection from a horizontal surface in a porous medium with Newtonian heating. Journal of Porous Media, 3(3): 227-235.
13. Lesnic, D., D. Ingham, I. Pop and C. Storr, 2004. Free convection boundary-layer flow above a nearly horizontal surface in a porous medium with Newtonian heating. Heat and mass transfer, 40(9): 665-672.
14. Salleh, M.Z., R. Nazar and I. Pop, 2010a. Modeling of free convection boundary layer flow on a solid sphere with Newtonian heating. Acta Applicandae Mathematicae, 112(3): 263-274.
15. Salleh, M.Z., R. Nazar and I. Pop, 2010b. Mixed convection boundary layer flow about a solid sphere with Newtonian heating. Archives of Mechanics, 62(4): 283-303.
16. Salleh, M.Z., R. Nazar and I. Pop, 2012. Numerical solutions of free convection boundary layer flow on a solid sphere with Newtonian heating in a micropolar fluid. Meccanica, 47(5): 1261-1269.
17. Salleh, M.Z., R. Nazar and I. Pop, 2010c. Mixed convection boundary layer flow from a solid sphere with Newtonian heating in a micropolar fluid. SRX Physics, doi:10.3814/2010/736039
18. Aziz, A., 2009. A similarity solution for laminar thermal boundary layer over a flat plate with a convective surface boundary condition. Communications in Nonlinear Science and Numerical Simulation, 14(4): 1064-1068.
19. Ishak, A., 2010. Similarity solutions for flow and heat transfer over a permeable surface with convective boundary condition. Applied Mathematics and Computation, 217(2): 837-842.
20. Ishak, A, N. Yacob and N. Bachok, 2011. Radiation effects on the thermal boundary layer flow over a moving plate with convective boundary condition. Meccanica, 46(4): 795-801.
21. Merkin, J. and I. Pop 2011 The forced convection flow of a uniform stream over a flat surface with a convective surface boundary condition. Communications in Nonlinear Science and Numerical Simulation, 16(9): 3602-3609.
22. Yao, S., T. Fang and Y. Zhong, 2011. Heat transfer of a generalized stretching/shrinking wall problem with convective boundary conditions. Communications in Nonlinear Science and Numerical Simulation, 16(2): 752-760.
23. Mohamed, M., M.Z. Salleh, R. Nazar and A. Ishak, 2013. Numerical investigation of stagnation point flow over a stretching sheet with convective boundary conditions. Boundary Value Problems, 2013(1): 1-10.
24. Cebeci, T. and P. Bradshaw, 1988. Physical and computational aspects of convective heat transfer. Springer, New York
25. Jena, S. and M. Mathur, 1981. Similarity solutions for laminar free convection flow of athermomicropolar fluid past a non-isothermal vertical flat plate. International Journal of Engineering Science, 19(11): 1431-1439.
26. Guram, G. and A. Smith, 1980. Stagnation flows of micropolar fluids with strong and weak interactions. Computers and Mathematics with Applications, 6(2): 213-233.
27. Ahmadi, G., 1976. Self-similar solution of imcompressible micropolar boundary layer flow over a semi-infinite plate. International Journal of Engineering Science, 14(7): 639-646.